



**Attached and  
unattached radon  
progeny, humidity and  
air temperature data in  
Jabiru East and Jabiru  
town: QUT-eriss  
project data**

F Quintarelli

RA Akber

J Pfitzner

July 1998

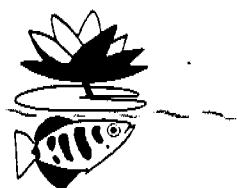


*supervising scientist*

Attached and Unattached Radon Progeny, Humidity and  
Air Temperature Data in Jabiru East and Jabiru Town:  
QUT-ERISS Project Data



Frank Quintarelli, Riaz Akber  
Centre for Medical and Health Physics  
Queensland University of Technology  
GPO Box 2434, BRISBANE Q 4001



John Pfitzner  
Environmental Research Institute of the Supervising Scientist  
PMB 2, JABIRU NT 0886

## Introduction

This report describes the data obtained over a period of 2 years starting in mid 1992 and ending in mid 1994 at Jabiru Town and Jabiru East, two sites in tropical Australia. The data consisted of the attached and unattached radon progeny. The study is relevant since the sites are located in Kakadu National Park, a popular tourist destination and in close proximity to ERA Ranger uranium mine as evident from Fig. 1.

The importance of the study stems from the fact that the radiotoxicity to humans depends on the size of the aerosol to which the radon progeny are attached. The unattached progeny are those decay products which are attached to very small aerosols. Because of their small size, these particles behave in much the same way as gas particles and are capable of penetrating deeply into the human respiratory tract. The attached progeny consist of progeny which are attached to aerosols which, because of their large size, behave more as dust particles, consequently, these do not penetrate as far into the respiratory tract. There is no clear distinction (in terms of their sizes) between attached and unattached progeny. For this study, the division is set at about 2.8  $\mu\text{m}$ , the aim being to mimic the deposition processes in the human respiratory tract.

## Instrumentation - Description and Theory of Operation

The data discussed in this report were obtained using a two channel diffusion battery. One channel consisted of a filter paper collector and a detector, whilst the second channel utilized a screen collector. The filter is totally absorbing - ie it collects the attached and unattached progeny, thus giving an estimate of the total activity in the atmospheric environment. The second channel uses a 200 mesh screen as the collector. As the air sample flows through the screen, the smaller aerosols have a higher probability of attaching to the screen because of their higher brownian motion. The larger aerosols exhibit a smaller degree of random motion, consequently these tend to follow the laminar streamlines of the airflow as it flows through the screen and have a much smaller likelihood of attaching to the screen.

The distinction between "large" and "small" aerosols is not ideally sharp, consequently it is customary to define a *cutoff particle diameter* as the diameter where a given fraction of particles are collected by the screen. The particle cutoff diameter is analogous to the cutoff frequency for an electronic filter. The cutoff diameter depends on factors such as the dimensions of the mesh, the characteristics of the air (presence of turbulence, temperature - and hence viscosity) and the sampling face velocity (the airspeed through the mesh).

The equations relating the fraction  $\eta$  of aerosols or particles collected by a screen to the particle diameter is (Ramamurthi and Hopke, 1989):

$$\eta = 1 - \exp\left\{-\frac{(4)(2.7)KVF^{-2/3}D^{2/3}}{\pi}\right\} \quad \text{Eq. 1}$$

where

$$KVF = \frac{U}{WF^{3/2}} \quad \text{Eq. 2}$$

$$WF = \frac{\alpha t}{(1-\alpha)w^{5/3}} \quad \text{Eq. 3}$$

$$D = \frac{kTC}{3\pi\mu d} \quad \text{Eq. 4}$$

$$C = 1 + \frac{\lambda}{d} \left( 2514 + 0.8 \exp\left\{-0.55 \frac{d}{\lambda}\right\} \right) \quad \text{Eq. 5}$$

where

T is the temperature in Kelvin

d is the particle diameter

k is Boltzman's constant (=  $1.37 \times 10^{-16}$  ergs/K)

$\lambda$  is the mean free path in air (=  $0.65 \times 10^{-5}$  cm)

$\mu$  is the viscosity of the air (=  $1.83 \times 10^{-4}$  gm cm/s)

U is the air speed through the mesh

w is the wire diameter

t is the screen thickness

$\alpha$  is the volume fraction

The above equations break down for particle diameters less than about 1.75 nm, however, the following correction for small particle diameters can be included in Eq. 5.

$$d^* = d \left( 1 + 3 \exp\{-2.20 \times 10^7 d\} \right) \quad \text{Eq. 6}$$

A convenient means of parameterising the collection characteristics of a screen is to specify the particle diameter at which 50 percent of particles are collected. Given this constraint, Eq. 1 becomes

$$d = 10^7 \exp \left\{ - \frac{32.193 + \ln(KVF)}{1.957} \right\} \quad \text{Eq. 7}$$

This equation is valid for  $0.001 < KVF < 0.325$ . It should also be noted that the constants in the above equation are in CGS units, consequently all input parameters for these equations should be in CGS units.

The operating parameters for the diffusion battery are summarised in Table 1. It should be noted that the height of the inlets is 1.5 m, approximating the height of the nasal cavity. Table 2 which summarises the screen parameters for the two channel diffusion battery used in this study.

### Description of the databases

The data consisted of files of half-hourly counts of radon progeny obtained using the two-channel sampler. These counts, along with the date and time, were stored in the file as half hour records. The data were collected over a two year period starting mid 1992 and finishing mid 1994. As data from two sites were recorded, the equipment was shared between these sites, resulting in observations from each site on alternate fortnights (approximately). The amount of data collected at each site for all the months in the study period are summarised in Table 3. For ease of manipulation, the data from each site were compiled into yearly databases consisting of 48 records per day for each of 31 days per month for twelve months. By allocating 31 days for each month (even though five have less), developing algorithms for searching for specific records and searching per se is expedited significantly since simple and fast arithmetic routines can be used to quickly locate any record in the database.

The data record format for the radon progeny counts is as follows:

ddmmyy hhmm t\* u\*

where

ddmmyy = the date - 2 digits for each of the day (dd), month (mm) and year (yy)

hhmm = the time - 2 digits for each of the hour (hh) and minutes (mm)

t\* = total progeny count (one or more digits)

u\* = unattached progeny count (one or more digits)

For example, the record "010393 2230 360 42" signifies that 22:30 hours on 01 March 1993 the total progeny count was 360 counts and the unattached count was 42.

Instances where no data were available were represented by the following "missing data" record:

-999999 -9999 -99 -99

The data record format for the meteorological observations is as follows:

ddmmyy hhmm h\* t\* p\*

where

ddmmyy = the date - 2 digits for each of the day (dd), month (mm) and year (yy)

hhmm = the time - 2 digits for each of the hour (hh) and minutes (mm)

h\* = relative humidity in percentage (one or more digits)

t\* = temperature in degrees Celsius (one or more digits)

p\* = barometric pressure in millibars (one or more digits)

For example, the record "010393 2230 70 42 1010" signifies that 22:30 hours on 01 March 1993 the relative humidity was 70%, the temperature was 42 degrees and the barometric pressure was 1010 millibars.

Instances where no data were available were represented by the following "missing data" record:

-999999 -9999 -99 -99 -99

The additional records which were included for months containing less than 31 days were also represented by the above "missing data" record.

It should be noted that a diurnal variation of about 25 mb was observed in the barometric pressure. Given the expected variation should have been about 2.5 - 3 mb, conversations with an experienced meteorologist and ERISS personnel indicated that the pressure sensor amplifier was probably set to a gain of ten instead of unity. The original database was, however maintained, and for the purpose of a preliminary review a correction was implemented in the analysis program.

Only the observed data were compiled into the databases. All other derived quantities, for example, the Potential Alpha Energy Concentration (PAEC), were calculated as they were required - which meant usually when a record was retrieved from the database. Advantages associated with this approach were that the databases possessed

a very simple structure, a minimum of data were stored in the database and the same retrieval software could be used on all databases - irrespective of whether these were radon progeny data or meteorological data from either Jaboru Town or Jaboru East. The perceived disadvantages were firstly, since data were available for 50% of the time, one half (on average) of the records were "missing data" records and secondly that derived quantities were calculated every time they were required - unnecessarily increasing computation time. Given today's hard disk sizes and computer speeds, neither of these proved to be a drawback.

### Data processing

The total and unattached PAECs were determined using the following relations:

$$ATTACHED\_PAEC = \frac{front\_total \times coll\_eff_1 \times E1 - E2}{front\_total \times coll\_eff_1 - coll\_eff_{100}} \quad \text{Eq. 8}$$

$$UNATTACHED\_PAEC = \frac{E2 - front\_total \times coll\_eff_{100} \times E1}{plate\_out(front\_total \times coll\_eff_1 - coll\_eff_{100})} \quad \text{Eq. 9}$$

$$TOTAL\ PAEC = ATTACHED\ PAEC + UNATTACHED\ PAEC$$

$$E1 = \frac{count_1 \times MeV\_eff}{det\_eff_1 \times conv\_factor \times flow_1 \times interval} \quad \text{Eq. 10}$$

$$E2 = \frac{count_2 \times MeV\_eff}{det\_eff_2 \times conv\_factor \times flow_2 \times interval} \quad \text{Eq. 11}$$

where

count1 = counts detected in channel 1 of the sampler

count2 = counts detected in channel 2 of the sampler

det\_eff1 = efficiency of detector 1 (= 0.123)

det\_eff2 = efficiency of detector 2 (= 0.121)

flow1 = flow rate through channel 1 (= 3.99 litres/minute)

flow2 = flow rate through channel 2 (= 3.92 litres/minute)

coll\_eff1 = collection efficiency of a screen for 1 nm aerosols (= 0.969)  
coll\_eff100 = collection efficiency of a screen for 100 nm aerosols (= 0.012)  
conv\_factor = counts to MeV conversion factor (= 130000)  
front\_total = front to total ratio - used if collector is a screen (= 0.82)  
MeV\_eff = Effective energy (in MeV) of emitted alpha particles (= 7.5)  
plate\_out = plate out factor (= 0.475)  
interval = duration of sampling interval in minutes (= 30)

These equations are essentially those derived at the Australian Radiation laboratories and also used by ERISS.

### **Data reduction**

The meteorological parameters recorded for the study and analysed included the temperature, relative humidity. Barometric pressure was investigated but the extensive data reduction has yet to be performed. The total quantity of data recorded over the study period amounted to about six months. Data were recorded approximately on alternate fortnights in Jabiru East and Jabiru Town. Since meteorological conditions do not vary significantly over small distances, if required, the Jabiru East and Jabiru Town data sets can be compiled into one more complete database for the overall area.

The diurnal variations in temperature and humidity are what one would normally expect for a tropical location - the temperature reaches a minimum value just before sunrise at about 0700h (local time) and a maximum at about 1600h. The diurnal variations in humidity reflect the temperature variations - attaining a maximum value when the temperature attains its minimum value and vice-versa.

Diurnal variations in temperature range from the low to mid twenties to a maximum in the mid thirties. Humidity ranges from about 20 to 50 percent in the dry season to 30 to 90 percent in the wet season.

The radon progeny parameters of interest in this study were the Total and Unattached PAEC and the Unattached Fraction. As these parameters were recorded on a half-hourly basis, the data were reduced by obtaining half-hourly averages for a calendar month at each site.



## **Diurnal behaviour of Total PAEC**

The prominent feature to note is the early morning peak, evident in Fig. 2, which reaches a maximum value at about 0800 hours. This peak is present most months and is believed to be caused by the build-up of radon in the stable early morning boundary layer. At sunrise, insolation gives rise to turbulence, which rapidly dissipates radon and its progeny.

A second and interesting feature in Fig. 2 is the occasional appearance of a peak in activity at about 2100 hours. For example, this peak is present during May 1994, however it is absent for the same month in 1993 as is evident in Fig. 3. To date there are insufficient supplementary meteorological data available to identify the cause of this peak; however, a plausible explanation is that this feature is not an isolated peak but the start of the following day's build-up. If this is the case, the valley between the peaks is in fact a dip embedded in a larger peak. Possible explanations for this dip in activity at about midnight include katabatic winds or the appearance of a low level jet, both of which give rise to mechanical turbulence, which would dissipate the airborne radioactivity.

The behaviour of Total PAEC between Jabiru East and Jabiru Town is similar, the only distinction between the two sites being that the activity at Jabiru East is consistently higher than Jabiru Town by about 50%.

## **Diurnal behaviour of Unattached PAEC**

The diurnal behaviour of the unattached PAEC (Fig. 4) closely mimics the behaviour of the total PAEC, the chief difference being its magnitude - which is generally an order of magnitude lower than the total PAEC. All comments regarding total PAEC also apply to the unattached PAEC.

## **Diurnal behaviour of Unattached Fraction**

The Unattached Fraction does not exhibit the marked variations which are characteristic of the total and unattached PAEC readings. The only trend is that for about 50% of cases, this parameter tends to be lower in the morning (between 0300 and 0900 hours) than in the mid afternoon as shown in Fig. 5. This behaviour is consistent with the hypothesis that during this period of the day the relative humidity is at its highest facilitating the formation of condensation nuclei. The converse occurs in mid-afternoon when the highest temperatures are observed. During this period, the higher temperatures result in lowered relative humidity and a lower amount of condensation nuclei. The graphs of unattached fraction exhibit a degree of variability, which compares with the magnitude of the diurnal variation, consequently, the diurnal

variation in some cases is not discernible. The diurnal variation however, does manifest itself clearly upon averaging an entire year's data.

### **Behaviour of Unattached PAEC and Unattached Fraction vs Total PAEC**

The seasonal variation in the behaviour of these parameters is very pronounced in the monthly scatter plots of Unattached PAEC vs. Total PAEC and Unattached Fraction vs Total PAEC (Figs. 6 and 7 respectively). During the wet season general trend is that the Unattached PAEC is linearly related to the Total PAEC with the correlation between these decreasing for the higher values of Total PAEC. The Unattached Fraction for the corresponding data set follows an inverse relationship - ie higher range of values in Unattached Fraction for low Total PAEC dropping off to consistently small values for the higher Total PAEC.

During the dry season, the linear relationship between Unattached and Total PAEC (Fig. 8) is not as well defined as in the wet season, the difference being in the greater degree of scatter at higher values of Total PAEC. The scatter plot of Unattached Fraction vs Total PAEC shown in Fig. 9 does not appear to display any significant behaviour or trends for this season, although there is still some resemblance to wet season behaviour.

### **Concluding Comments**

Preliminary interpretation thus far have revealed that the concentrations of Total and Unattached PAEC and Unattached Fraction exhibit diurnal and seasonal behaviour. Also the behaviour varies markedly for the same month in different years. In summary, these interpretations have revealed that:

- \* The total and unattached PAEC are strongly dependent on whether it is the wet or dry season - ie the presence of aerosols other than moisture droplets (eg smoke particles from bushfires) strongly influence PAEC behaviour. However one should not rule out the possibility that the humidity may also influence the behaviour of these aerosols.

- \* The appearance of the scatter plots depends on season as mentioned above.

- \* The position of the morning peak in total PAEC appears to depend on the season, ranging from about 0600h in the dry to about 0900 in the wet season. A possible explanation is that moisture in the form of surface water may keep temperatures low until it has evaporated, thus delaying the onset of convective activity which dissipates the radionuclides which accumulated during the stable night-time regime.

\* There is a marked variation in behaviour of radon progeny for the same month but different years, possibly indicating that the available observations are a subset of a much larger and varied superset.

\* The aerosol behaviour, the factors affecting aerosol behaviour, and, to a lesser extent the meteorology, are not fully understood.

\* The interaction between Radon progeny, aerosol and meteorology are not fully understood.

The entire data are available on a CD ROM enclosed in this report. The plots of monthly averages are included as an Appendix which may be viewed in ERISS File JC1236.

#### References

Ramamurthi, M and Hopke PK, (1989), On improving the validity of wire screen "unattached" fraction Rn daughter measurements. *Health Physics*, **56**, 189-194

**Table 1. Operating parameters for the diffusion battery used in this study.**

Parameter	Value
Mesh Size	200
Mesh Diameter	40 mm
Mesh Volume Fraction	0.291
Mesh Thickness	80 $\mu\text{m}$
Mesh Wire Diameter	35 $\mu\text{m}$
Cutoff Particle Diameter (50% Collection)	2.82 nm
Collection Efficiency at 1 nm	96.9 %
Collection Efficiency at 100 nm	1.2 %
Sampling Face Velocity	17.7 cm/s
Sampling Rate	4 L/min (nominal)
Height of Inlet Above Ground	1.5 m

**Table 2. Parameters for wire screen used in this study.**

Mesh Number	Wire Diameter	Screen Thickness	Volume Fraction	Wire Spacing
200	35 $\mu\text{m}$	80 $\mu\text{m}$	0.291	125 $\mu\text{m}$

**Table 3. Summary of available Radon and Meteorology data on a monthly basis.**

**Radon progeny data for 1992**

**Jabiru East**

<b>Month</b>	<b>Days</b>	<b>Records</b>
January	0	0
February	0	0
March	0	0
April	0	0
May	0	0
June	0	0
July	5	204
August	15	626
September	4	149
October	14	500
November	15	519
December	17	742

**Jabiru Town**

<b>Month</b>	<b>Days</b>	<b>Records</b>
January	0	0
February	0	0
March	0	0
April	0	0
May	0	0
June	0	0
July	0	0
August	19	868
September	24	1102
October	2	43
November	14	629
December	6	253

## Radon progeny data for 1993

### Jabiru East

Month	Days	Records
January	24	1092
February	2	80
March	14	634
April	11	454
May	14	468
June	9	355
July	12	527
August	9	365
September	17	701
October	16	633
November	15	644
December	14	555

### Jabiru Town

Month	Days	Records
January	11	469
February	23	1066
March	2	81
April	10	398
May	8	342
June	9	371
July	0	0
August	4	136
September	14	619
October	13	554
November	15	659
December	15	612

## Radon progeny data for 1994

### Jabiru East

Month	Days	Records
January	4	147
February	5	152
March	16	668
April	0	0
May	22	952
June	2	91
July	0	0
August	0	0
September	0	0
October	0	0
November	0	0
December	0	0

### Jabiru Town

Month	Days	Records
January	0	0
February	14	569
March	14	582
April	19	828
May	0	0
June	16	710
July	6	248
August	0	0
September	0	0
October	0	0
November	0	0
December	0	0

## Available meteorological data for 1992

### Jabiru East

Month	Pressure (days)	Pressure (records)	Temperature (days)	Temperature (records)	Humidity (days)	Humidity (records)
January	0	0	0	0	0	0
February	0	0	0	0	0	0
March	0	0	0	0	0	0
April	0	0	0	0	0	0
May	0	0	0	0	0	0
June	0	0	0	0	0	0
July	4	171	4	171	4	171
August	10	317	10	317	10	409
September	0	0	0	0	0	0
October	0	0	0	0	0	0
November	0	0	0	0	0	0
December	0	0	0	0	0	0

### Jabiru Town

Month	Pressure (days)	Pressure (records)	Temperature (days)	Temperature (records)	Humidity (days)	Humidity (records)
January	0	0	0	0	0	0
February	0	0	0	0	0	0
March	0	0	0	0	0	0
April	0	0	0	0	7	297
May	0	0	0	0	0	0
June	0	0	0	0	0	0
July	8	344	8	344	8	344
August	0	0	0	0	0	0
September	0	0	0	0	0	0
October	0	0	0	0	0	0
November	0	0	0	0	0	0
December	0	0	0	0	0	0



# **Available meteorological data for 1993**

## **Jabiru East**

<b>Month</b>	<b>Pressure (days)</b>	<b>Pressure (records)</b>	<b>Temperature (days)</b>	<b>Temperature (records)</b>	<b>Humidity (days)</b>	<b>Humidity (records)</b>
January	0	0	0	0	0	0
February	0	0	0	0	0	0
March	0	0	0	0	0	0
April	0	0	0	0	0	0
May	14	637	14	637	0	0
June	16	697	21	962	21	962
July	13	592	14	616	14	616
August	5	190	5	190	5	190
September	18	809	18	809	18	809
October	7	315	7	315	7	315
November	0	0	0	0	0	0
December	0	0	0	0	0	0

## **Jabiru Town**

<b>Month</b>	<b>Pressure (days)</b>	<b>Pressure (records)</b>	<b>Temperature (days)</b>	<b>Temperature (records)</b>	<b>Humidity (days)</b>	<b>Humidity (records)</b>
January	0	0	0	0	0	0
February	0	0	0	0	0	0
March	0	0	0	0	0	0
April	5	135	8	314	8	343
May	0	0	0	0	0	0
June	11	471	11	471	11	470
July	0	0	0	0	0	0
August	19	862	19	862	19	862
September	14	624	14	624	14	624
October	15	669	15	669	15	669
November	0	0	0	0	0	0
December	0	0	0	0	0	0

# Available meteorological data 1994

## Jabiru East

Month	Pressure (days)	Pressure (records)	Temperature (days)	Temperature (records)	Humidity (days)	Humidity (records)
January	0	0	0	0	0	0
February	0	0	0	0	0	0
March	0	0	0	0	0	0
April	0	0	0	0	0	0
May	15	692	15	692	15	692
June	8	356	8	356	8	355
July	0	0	0	0	0	0
August	0	0	0	0	0	0
September	0	0	0	0	0	0
October	0	0	0	0	0	0
November	0	0	0	0	0	0
December	0	0	0	0	0	0

## Jabiru Town

Month	Pressure (days)	Pressure (records)	Temperature (days)	Temperature (records)	Humidity (days)	Humidity (records)
January	0	0	0	0	0	0
February	0	0	0	0	0	0
March	0	0	0	0	7	297
April	0	0	0	0	0	0
May	0	0	0	0	0	0
June	0	0	0	0	0	0
July	0	0	0	0	0	0
August	0	0	0	0	0	0
September	0	0	0	0	0	0
October	0	0	0	0	0	0
November	0	0	0	0	0	0
December	0	0	0	0	0	0

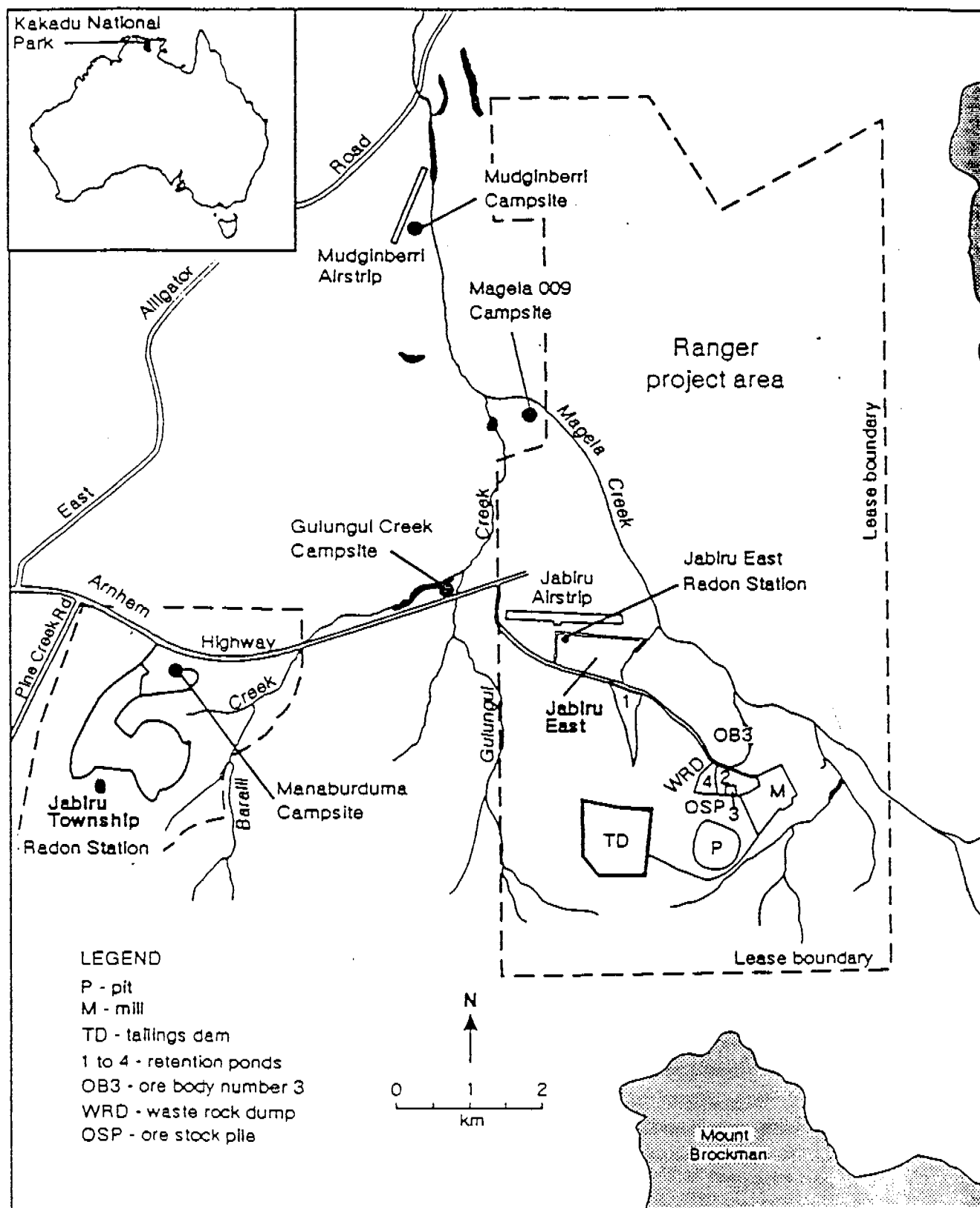


Figure 1: A locality map to identify the sampling locations.

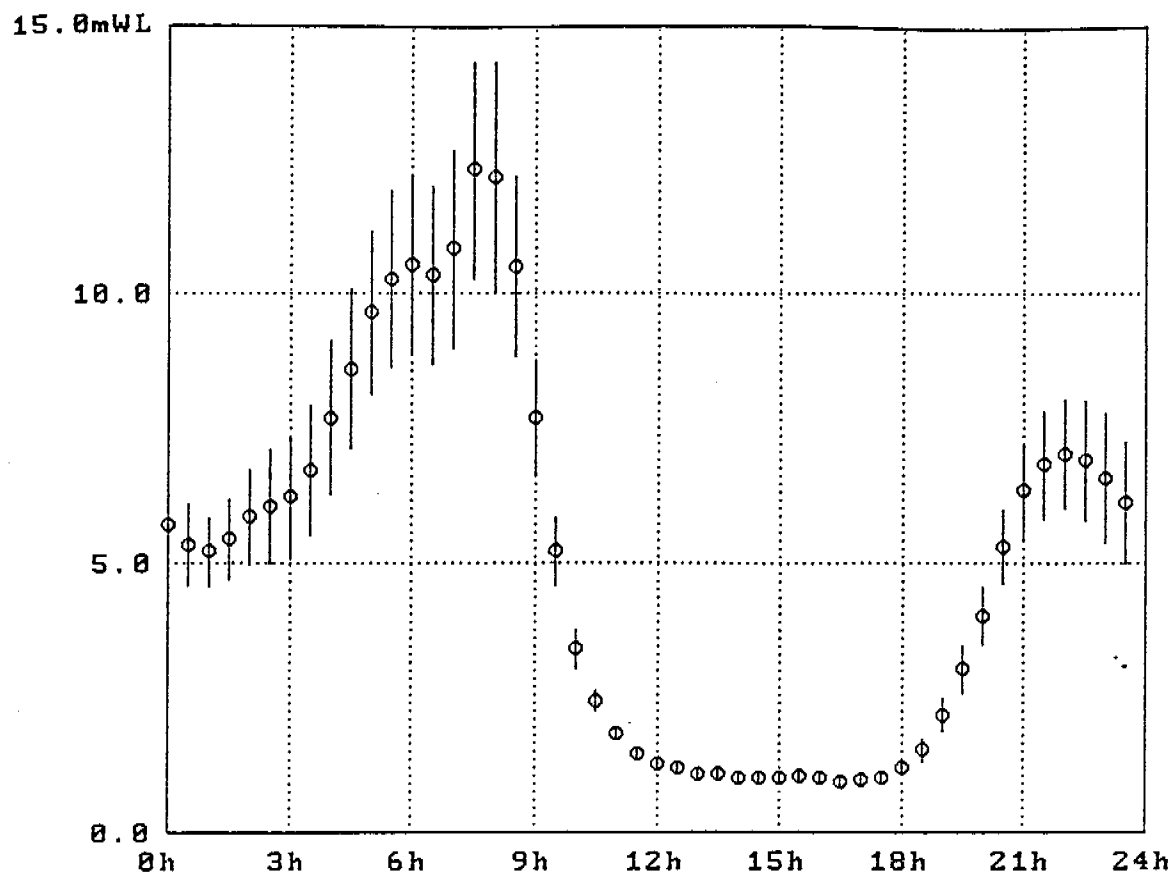


Figure 2: Total PAEC vs. Time of the Day; monthly average for May 1994 in Jabiru East.

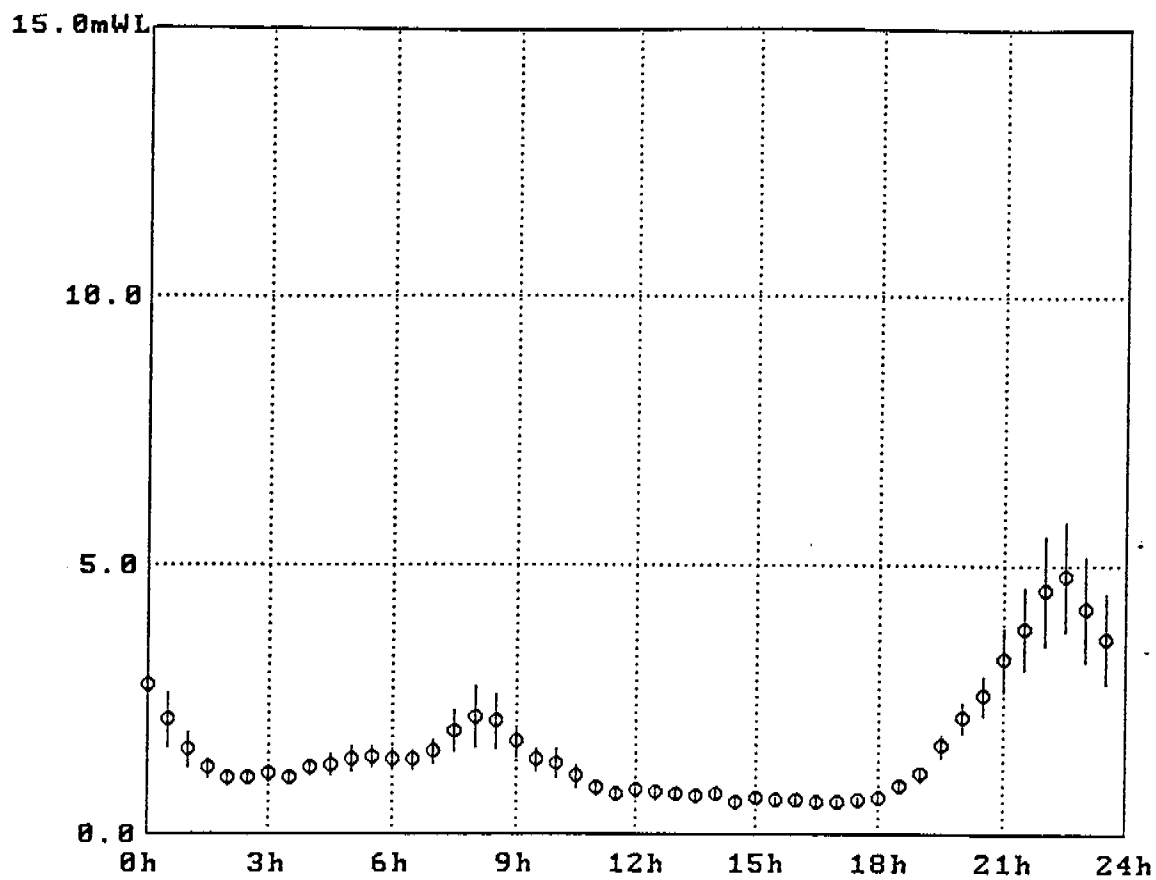


Figure 3: Total PAEC vs. Time of the Day; monthly average for May 1993 in Jabiru East.

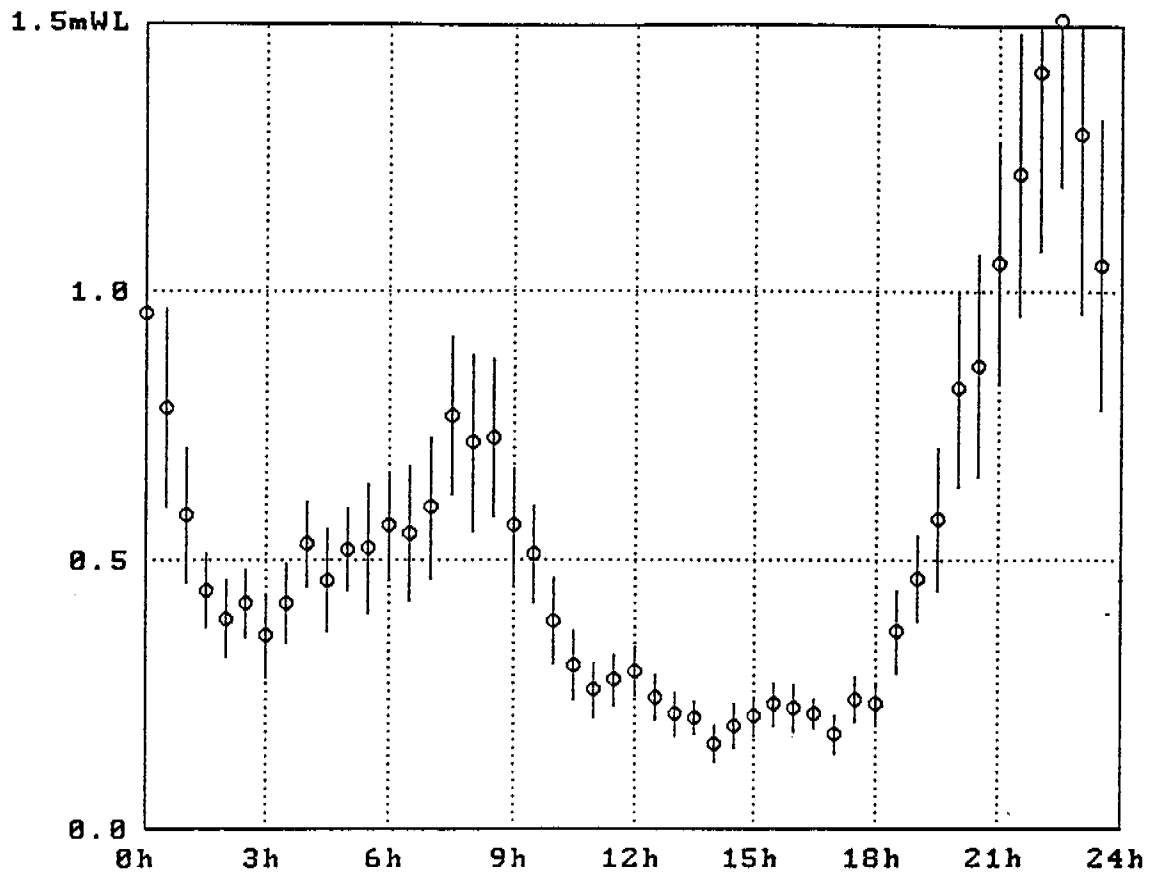


Figure 4: Unattached PAEC vs. Time of the Day; monthly average for May 1993 in Jabiru East.

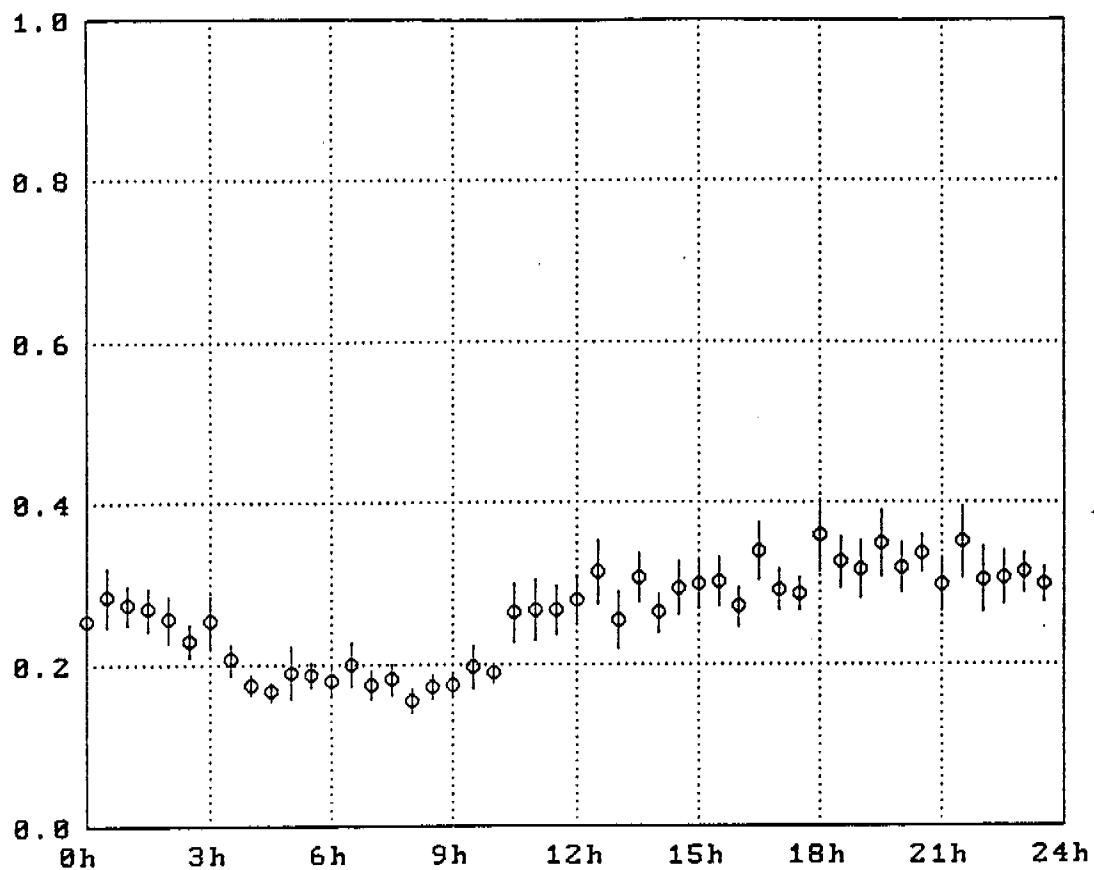


Figure 5: Unattached Fraction vs. Time of the Day; note a decrease in value during early morning when peaks occur in PAEC concentrations.

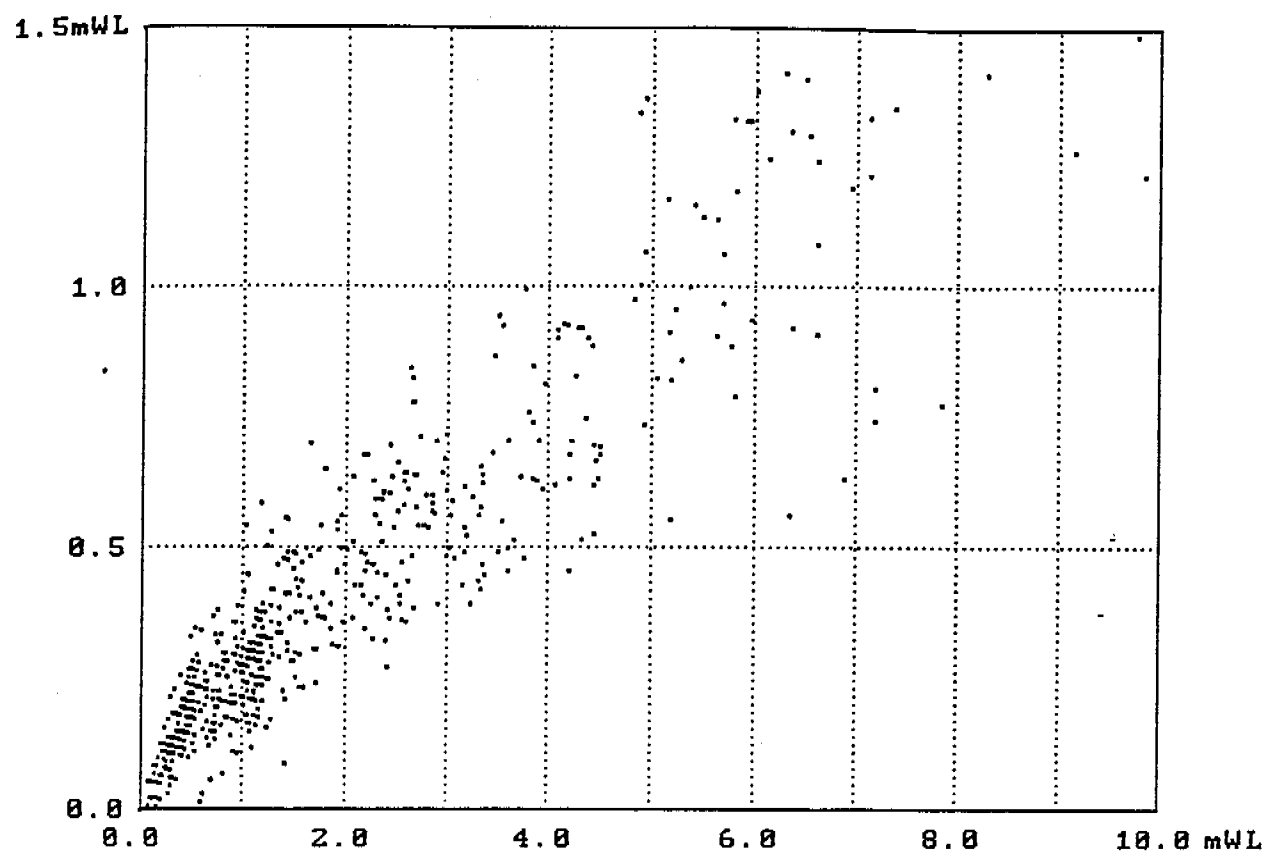


Figure 6: Scatter plot of Unattached PAEC vs. Total PAEC. The data are for Jabiru East, March 1993 and represent the Wet season behaviour.



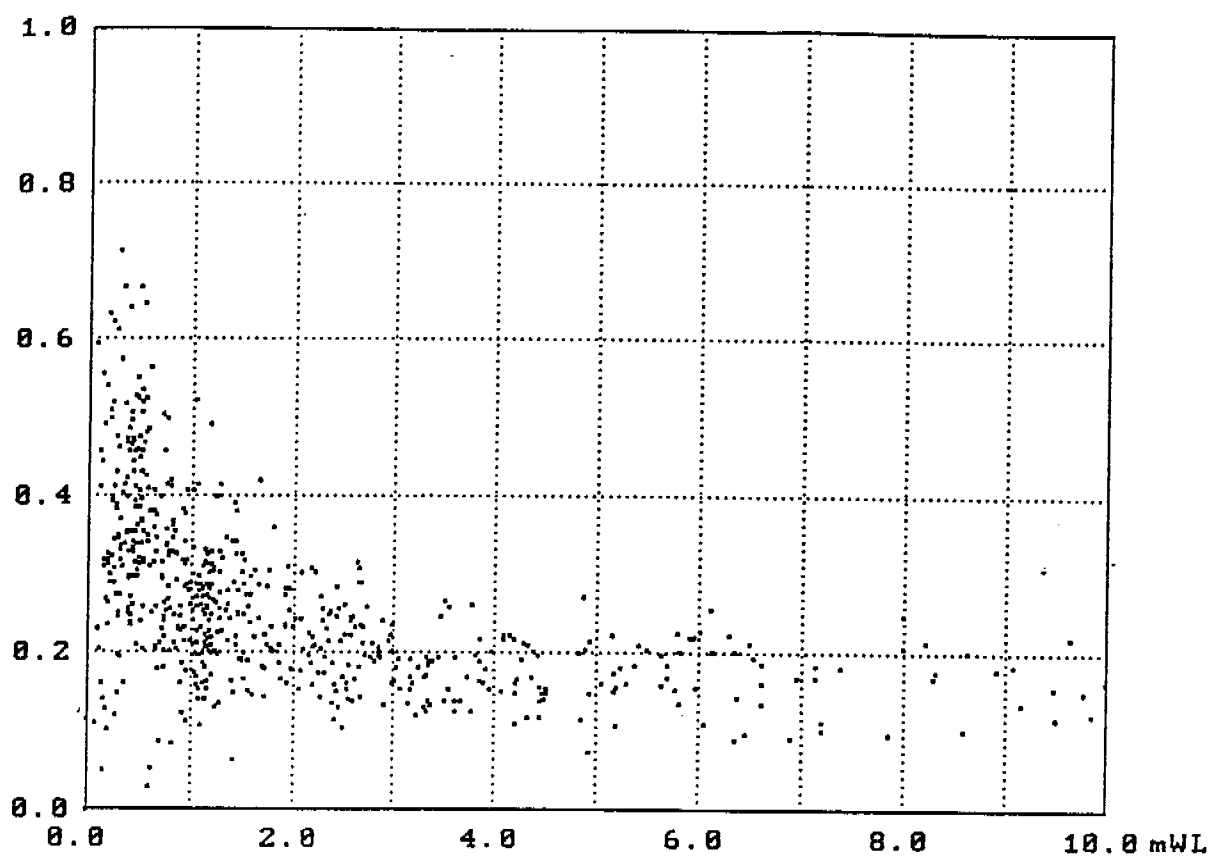


Figure 7: Unattached Fraction vs. Total PAEC for March 1993 in Jabiru East representing the Wet season behaviour.

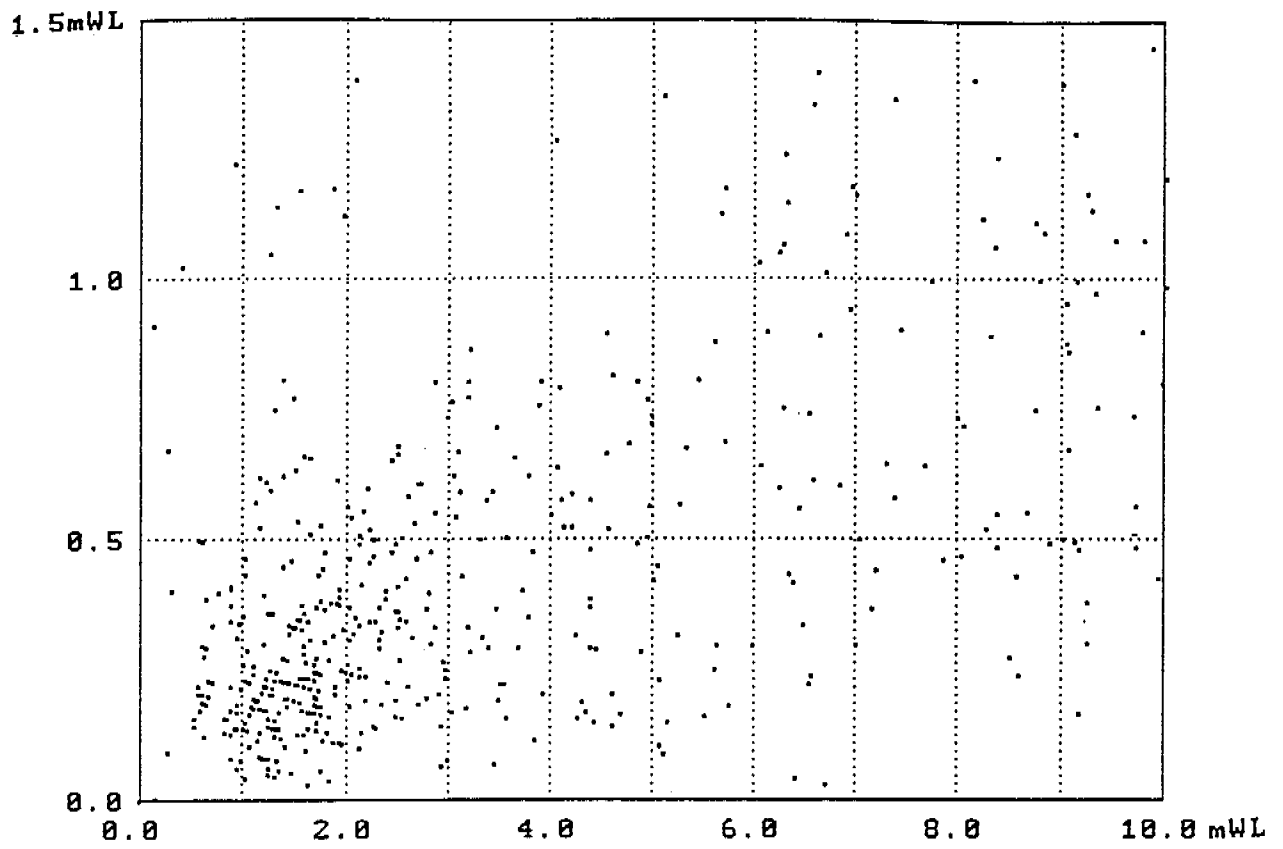


Figure 8: Unattached PAEC vs, Total PAEC scatter plot for July 1993, Jabiru East, Dry season.

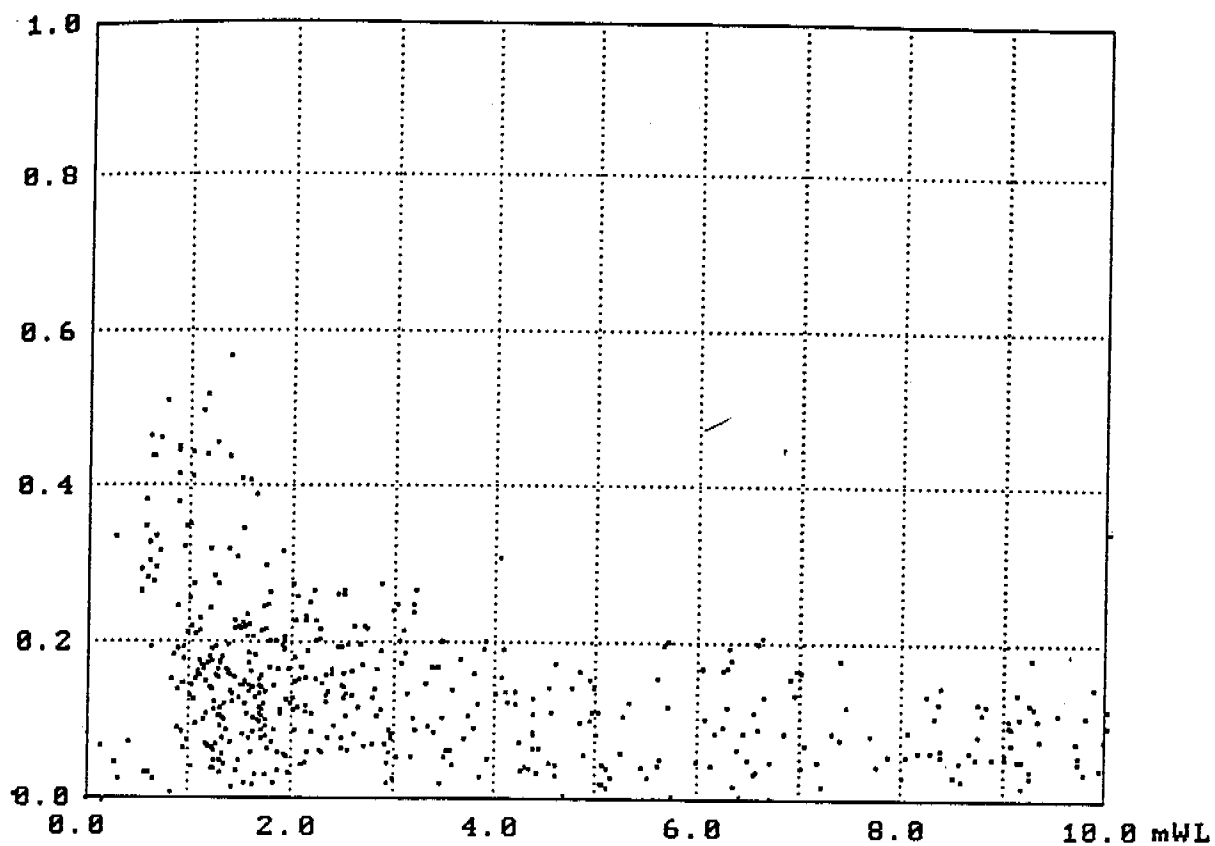


Figure 9: Unattached Fraction vs. Total PAEC scatter plot for Jabiru East in July 1993.